MULTIPLE PHASE-FORMATION IN Ni-Ge SYSTEM MONITORED BY SEM, AFM AND PIXE ANALYTICAL TECHNIQUES

Chilukusha Daniel[1*], Habanyama Adrian[1] and Mweene V. Habatwa[1]

[1]University of Zambia, Department of Physics, School of Natural Science, P.O. Box 32379, Lusaka 10101, Zambia

*Corresponding author: Tel: +260977307435

Abstract

We present evidence of multiple phase formation in the Ni-Ge system observed with the aid of the Scanning Electron Microscope (SEM), Atomic Force Microscope (AFM) and Particle Induced X-ray Emission (PIXE) analytical techniques. Using a conventional optical mask, we prepare lateral diffusion couples of thick rectangular germanium islands on a nickel thin film. We observe at elevated temperatures a lateral diffusion of excess atoms from the Ge rich island to the surrounding Ni thin film; in a process which leaves a sequence of clearly discernible multiple phases whose interfaces are optically resolvable. We reveal finer detail in structure, texture and stoichiometry of the phases using AFM and SEM micrographs together with μ-RBS (Microprobe Rutherford Backscattering Spectrometry) and μ-PIXE elemental distribution maps. Our results confirm that when complemented with AFM, SEM, and micro-Rutherford backscattering spectrometry, lateral diffusion coupling technique is the most effective method to observe simultaneously multiple phases in a metallic-semiconducting binary system.

INTRODUCTION

In recent years, germanium has attracted a significant amount of research interest due to its great potential to replace/compliment silicon as a material for ultra-fast nano-scale Complementary Metal Oxide Semiconductor (CMOS) transistors. Nickel germanides are viewed as the most suitable materials for use as ohmic contacts and interconnects. Implementation of germanium based technology will, however, require a thorough understanding of the solid state interactions in metal-germanium systems in order to foresee and avoid problems that may be encountered during integration. This study sets out to investigate the solid state interactions in the germanium-nickel system.

Thin film couples of nickel and germanium have been investigated previously, but the results are rather contradictory as different researches have reported differently on various aspects of phase formation. For instance, Gaudet *et al.* [1] and Nemouchi *et al.* [2] identified Ni_5Ge_3 as the first phase to form in the Ni-Ge system. This is consistent with the results reported by Habanyama *et al.* [3,4]. However, it is in contrast with the results of Marshal and others [5] which reported the formation of Ni_2Ge as the first phase to form in the Ni-Ge system. In another study conducted by Jin *et al.* [6], Ni_3Ge_2 was also reported as the first phase to form. These workers all reported the reactions to occur at temperatures of 150 ^oC and above. Whereas different authors have reported different phases as the first ones to be formed in the Ni-Ge system, there is a general consensus on NiGe being the second phase, which various workers have reportedly observed at temperatures between 200-600 ˚C.

Table 1 summarises the phase formation sequences and their typical formation temperatures as reported by different researchers.

Table 1: Survey on the study of phase transformation on the Ni/Ge system

No	First phase		Second phase		Reference
	Observed phase	Formation temperature (^oC)	Observed phase	Typical formation temperature (^oC)	
1	Ni_2Ge	≈ 250 160 150-300	NiGe	260-600 250 250-600	E.D. Marshal *et al.* [5] Y.F. Hsieh *et al.* [7] M.W. Wittmer *et al.* [8]
2	Ni_3Ge_2	-	NiGe	-	L.J. Jin *et al.* [6a]
3	Ni_5Ge_3	- - -	NiGe	- 150 200–300	S. Gaudet *et al.* [9b] F. Nemouchi *et al.* [2,10c] Patterson *et al.* [11] Habanyama *et al* [3,4]
4	Ni_5Ge_3/Ni_2Ge	250/300	NiGe	350	M. Mueller *et al.* [12d]

The Ni-Ge system has never been studied in the lateral diffusion couple regime.

EXPERIMENTAL

Si (100) wafers were thermally oxidised after which they were cut into approximately 0.5 cm squares and ultrasonically cleaned with organic solvents. They served as substrates (substrate = Si<100>/SiO_2(4000 Å)). Layer deposition was done using electron beam vacuum evaporation in a pressure of 10^{-7} mbar. Prior to preparation of the lateral diffusion couple samples, a preliminary investigation of the Ni-Ge system was done using conventional thin films for comparison purposes. The sample structures used for the preliminary study had 500 Å of nickel and 3000 Å of germanium sequentially deposited on oxidised silicon. A thin layer of titanium (~10 Å) was deposited onto the SiO_2 prior to the deposition of the Ge. It is important to note that the Ti in this experiment was not used as an inert marker, but rather as a 'glue' to make the structure adhere. Some of the samples were isothermally annealed to activate solid-state interactions and subsequently characterized using ordinary *ex-situ* RBS. In addition, one sample was annealed *in-situ*, while ramping temperature, and monitored using RBS in real time.

Lateral diffusion couple samples were prepared by first depositing a thin film of one material on the substrate in much the same way as in conventional thin films. A silicon mask with an array of 780 × 390 μm windows was then brought into contact with the film without breaking the vacuum. The island material was deposited through the mask, resulting in structures consisting of nickel islands on germanium films and vice-versa. In both cases, the island materials had thickness 2000 Å while the thin films had 500 Å. The layer thicknesses were chosen such that the atomic ratio of island material to thin film was much greater than that of the most island-material rich phase of the Ni-Ge binary system. The samples were annealed under different conditions and later characterised using the

following techniques: Optical Microscopy, Atomic Force Microscopy, Scanning Electron Microscopy, Microprobe PIXE and Microprobe RBS.

THIN FILM RESULTS AND DISCUSSION

A. Results

Figure 1 shows an *ex-situ* RBS spectrum obtained from the as-deposited sample in the preliminary thin film investigation. The simulation of the spectrum, as obtained using a computer software package called RUMP, indicates the presence of a thin layer of Ni_5Ge_3 between the Ni and Ge layers. Since the sample had not yet been subjected to heat treatment, it can be inferred that the Ni_5Ge_3 was formed during deposition of the Ni and Ge films. According to Nemouchi *et al.* [10], it is possible for a daughter phase to nucleate during layer deposition due to the presence of the heat of condensation of the phases being deposited.

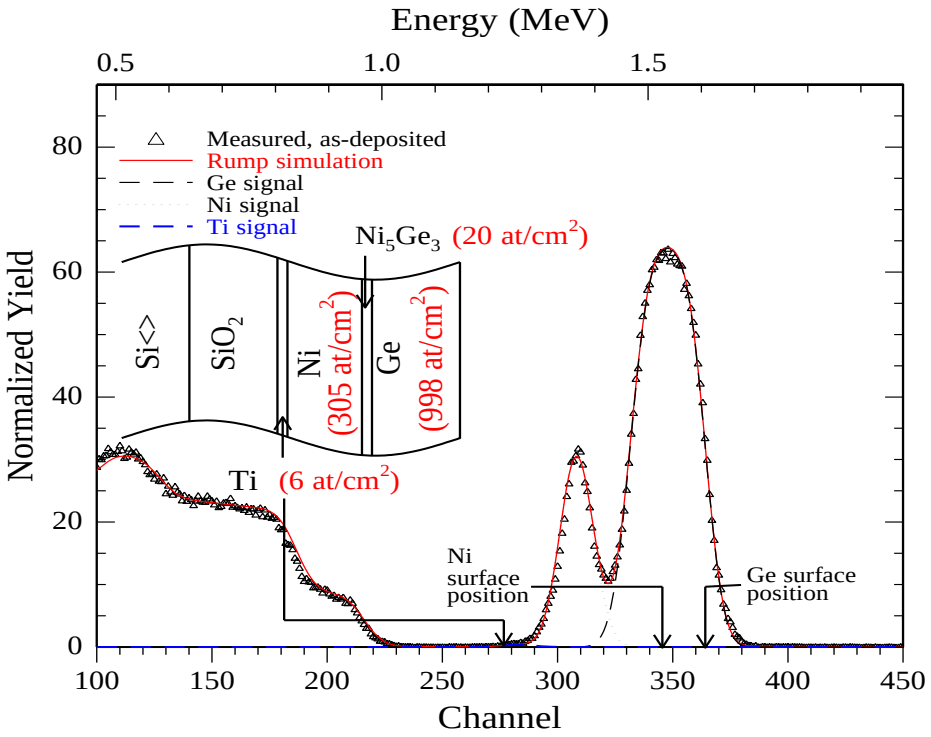

Figure 1: RBS spectrum and RUMP simulation of the as-deposited sample with configuration Si<100>/SiO_2/Ti(10 Å)/Ni(500 Å)/Ge(2000 Å). The sample exhibited some initial reactions that resulted in the formation of a thin layer of Ni_5Ge_3.

The RBS spectrum obtained from the sample that was isothermally annealed at 150 °C for 30 minutes is shown in Figure 2. The RUMP simulation of this spectrum did not show any major change in structure from that of the as-deposited sample. Thermal anneals at the same temperature but for longer times (1 and 2 hours) yielded a similar result, as evidenced by the other two spectra displayed in the figure.

When the system was isothermally treated at 300 °C for 2 hours, the compound phase NiGe was observed. Unreacted Ni was completely consumed while the thickness of the Ge layer was found to have reduced correspondingly.

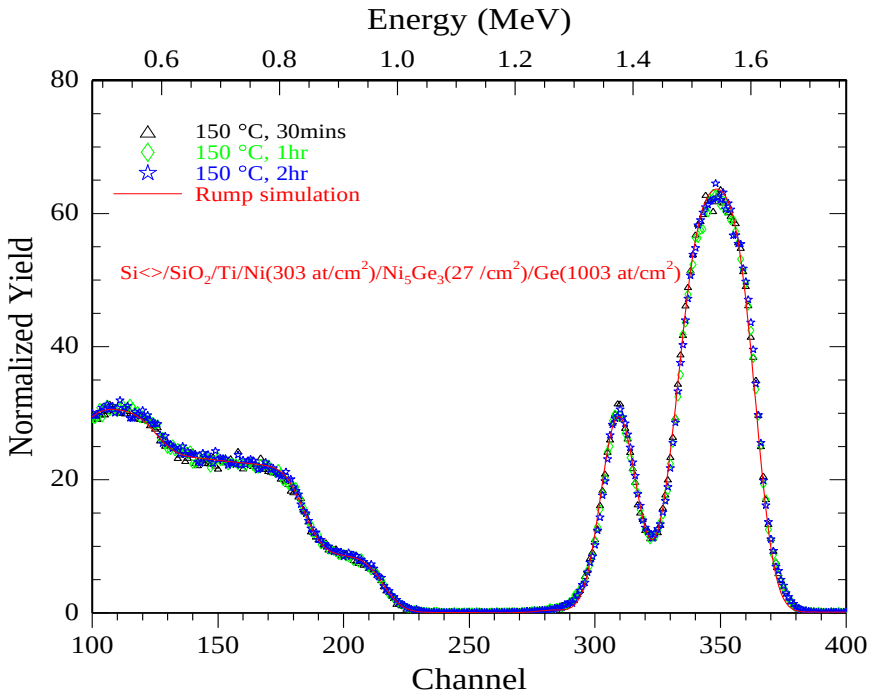

Figure 2: Overlays and RUMP simulation of spectra from the samples that were isothermally annealed at 150 °C for different anneal-times. The RUMP simulation showed that the composition of these samples was similar to that of the as-deposited sample.

RBS spectra obtained from samples that were treated at the same temperature for shorter anneal times showed no change in structure, as shown in Figure 3. The results from thin film couples that were isothermally annealed thus indicated that thermally induced interactions occurred in the temperature range between 150 and 300 °C. From these data, it was not possible to determine the exact temperature at which the interaction commenced as well as the formation temperatures for subsequent phases. All that could be established was that NiGe is the last phase to form in the system.

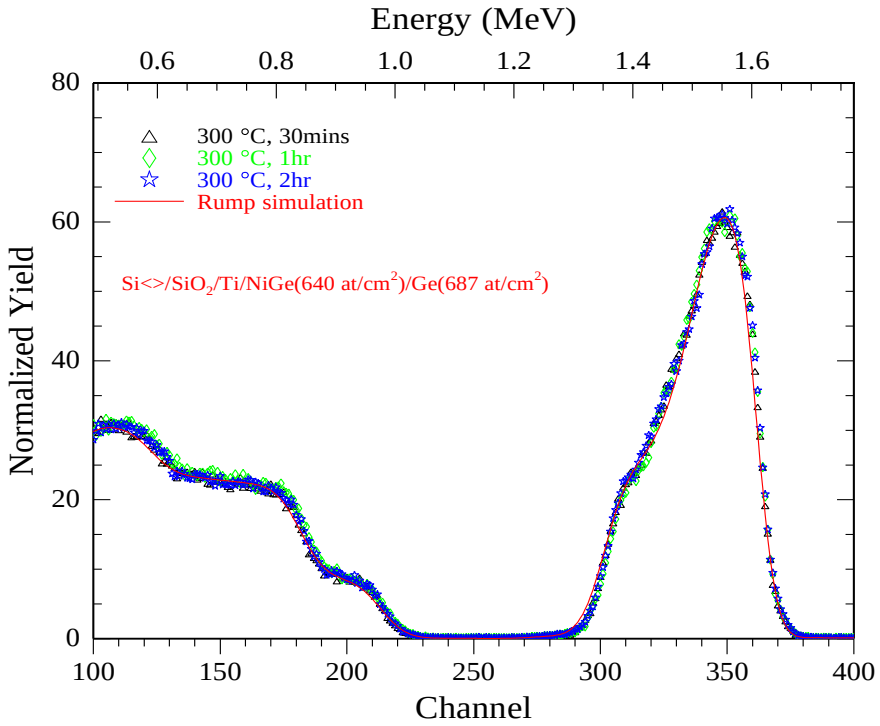

Figure 3: Overlays of RBS spectra obtained from samples isothermally annealed at 300 °C for different anneal-times. The RUMP simulation revealed that in these samples all the Ni had been consumed, which explains why the system had acquired stable equilibrium.

Since ordinary RBS could not indicate the precise temperature for the beginning of the thermally induced reactions in the Ni-Ge system, recourse was taken to *in-situ* real-time RBS. By recording sequential spectra of the system while ramping the temperature from 28 °C up to 500 °C, it was possible to study the entire evolution of the system in one experimental run. In Figure 4, RBS spectra obtained at selected stages of the reaction are superposed. The expected heights of the Ni peak for various Ni-Ge phases are also indicated in the figure. The height of the Ni signal in the spectrum obtained at 200 °C is slightly lower than the expected height of unreacted Ni, signifying that by this temperature, thermally induced reactions had already commenced. The peak height of the spectrum taken at 227 °C suggests the presence of the phase Ni_5Ge_3 while those obtained at 243 °C and 254 °C indicate the presence of NiGe. A spectrum acquired at a much higher temperature than 254 °C (285 °C) is included in Figure 4 as evidence that the reaction had reached completion.

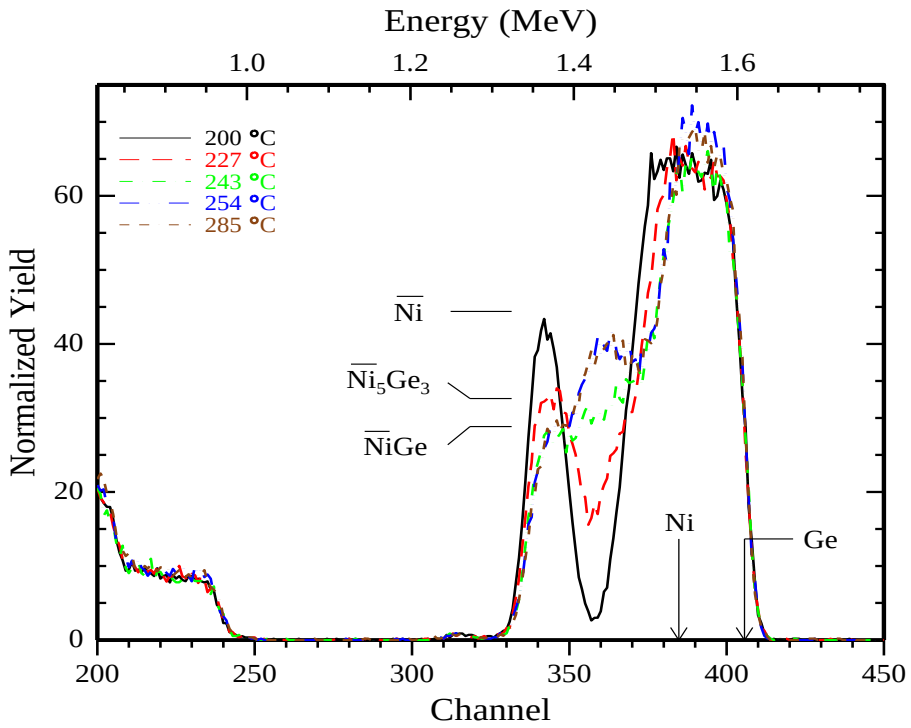

Figure 4: Superposition of RBS spectra obtained at selected stages of the in-situ reaction.

The collected RBS spectra were fitted using RUMP to obtain composition and layer-thickness information. A summary of the entire analysis is graphically presented in Figure 5. The *in-situ* RBS results confirmed the presence of the Ni_5Ge_3 layer that was observed in the as deposited sample with *ex-situ* RBS. The thickness of this layer remained constant until a temperature of about 150 °C, at which point heat-treatment induced interactions commenced with the continued growth of Ni_5Ge_3. The Ni_5Ge_3 layer grew steadily until a temperature of 223 °C when the second and last phase, NiGe, was detected. A short period of simultaneous growth of Ni_5Ge_3 and NiGe was observed in the temperature range 223 °C – 232 °C. During this time, the growth of Ni_5Ge_3 slowed down noticeably. After complete consumption of unreacted Ni at 232 °C, Ni_5Ge_3 decomposed as NiGe grew at its expense. The reaction came to an end at 254 ^{0}C after all the Ni_5Ge_3 had been consumed.

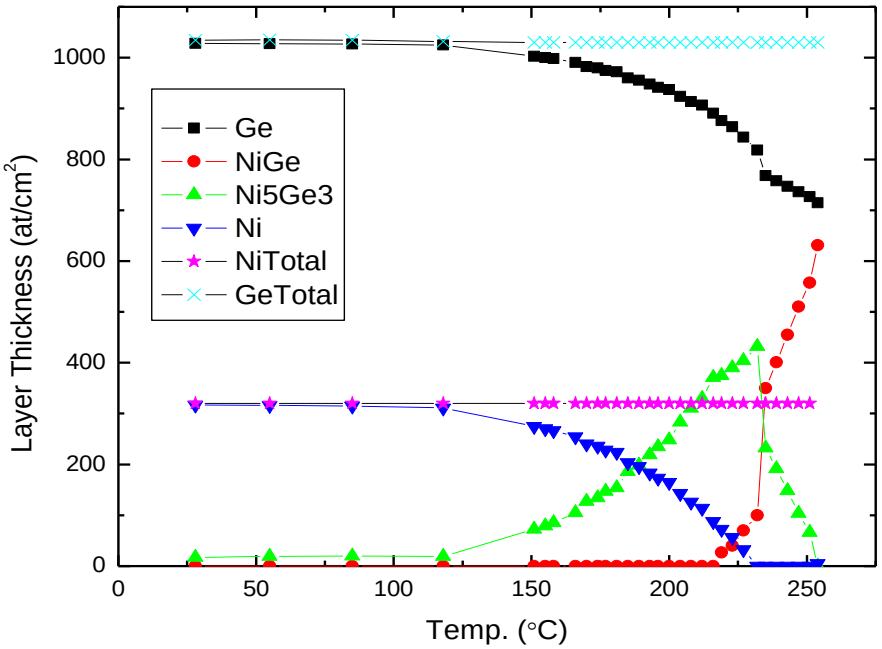

Figure 5: Phase formation and decomposition in the sample with configuration Si<100>/SiO_2/Ti(10 Å)/Ni(500 Å)/Ge(2000 Å) analysed using in-situ real-time RBS.

B. Analysis and Discussion (Thin Film Couples)

1. Phase Formation

In the samples with configuration Si<100>/SiO_2/Ti(10 Å)/Ni(500 Å)/Ge(2000 Å) that were treated isothermally at 150 °C, no major change was observed in the structure, meaning that thermally induced solid-state reactions had not yet commenced at that temperature. When the sample was annealed at 300 °C, it was found that all the reactions had occurred and the system had reached equilibrium. NiGe was the only compound phase detected in the samples. These observations are consistent with results obtained in previous experiments in the literature, (see Table 1) except for slight variations in temperatures of formation.

Results obtained from *in-situ* RBS showed that Ni_5Ge_3 was the first phase to form in the Ni-Ge binary system. A thin layer of this phase, suspected to have formed during deposition, was found to be already present in the sample before the beginning of temperature ramping. The thickness of this layer remained constant up to a temperature of 150 °C when its growth due to heat treatment commenced. The Ni_5Ge_3 layer grew steadily until 232 °C when all unreacted Ni was consumed. The second and last phase, NiGe, started to grow at 219 °C even before Ni was completely consumed, resulting in a short period of coexistence of Ni_5Ge_3 and NiGe in the presence of unreacted Ni.

A survey of the literature available as regards first phase formation showed that three phases, Ni_5Ge_3, Ni_2Ge, and Ni_3Ge_2 are usually reported as the first ones to form in the Ni-Ge system. Our observation of Ni_5Ge_3 is in agreement with the results obtained by Habanyama *et al.* [3,4], Nemouchi *et al.* [2,10], Gaudet *et al.* [9,13], and Mueller *et al.* [12]. In their *in-situ* RBS study of the Ni-Ge system, Habanyama *et al.* investigated samples with two

configurations: Ge<100>/Ta(5 Å)/Ni(800 Å) and Ge<100>/Ta(6 Å)/Ge(490 Å)/Ni(470 Å). The former indicated that the formation of Ni_5Ge_3 commenced at 145 °C and ended at around 298 °C, while the latter exhibited room-temperature reactions leading to formation of a layer of Ni_5Ge_3. This layer continued to grow until a temperature of 239 °C, when all the Ge above the Ta marker was consumed. Nemouchi *et al*. found that the formation of Ni_5Ge_3 occurred at 160 °C (using *in-situ* XRD) and at 175 °C (using TEM), while Gaudet *et al*. observed the same phase near an annealing temperature of 170 °C. Studies by Mueller *et al.* [12] indicated that Ni_5Ge_3 and Ni_2Ge are the Ni-rich phases that form below 350 °C. The groups of researchers that have identified $NiGe_2$ as the first phase to form include Marshal *et al.* [5], Hsieh *et al.* [14] and Wittmer *et al.* [8]. Their results are also consistent with the prediction of the Walser-Bene (W-B) rule that Ni_2Ge should form first in the binary Ni-Ge system. A study conducted by Jin *et al.* [6] reported Ni_3Ge_2 as the first germanide to form. These workers all reported the reactions to occur at temperatures above 150 ^oC.

The identification of NiGe as the second and final phase to form at 223 ^oC in the present study is in agreement with much of the published literature. Whereas different authors have reported different phases as the first ones to form in the Ni-Ge system, there is a general consensus on NiGe being the second phase (see Table 1.3). With the exception of Nemouchi *et al.* [10] who reported the formation of NiGe during deposition at room temperature, all the workers have reportedly observed NiGe at temperatures between 200 °C and 600 °C. Previous experiments whose results are in closest agreement with ours include those by Patterson *et al*. [11] and Habanyama *et al*. [3,4] which report the formation of NiGe at temperatures of 200 °C and 239 °C respectively. Others are those conducted by Hsieh *et al*. [14] in which NiGe was detected at 250 °C, and those by Wittmer *et al.* [8] and Marshal *et al.* [5] in which formation of NiGe was observed in the temperature ranges 250 – 600 °C and 260 –600 °C respectively. The identification of NiGe as the last phase is also in agreement with the Ni-Ge binary equilibrium phase diagram where it is predicted as the last and most Ge-rich phase to form in the Ni-Ge system.

The understanding of the processes that are responsible for the simultaneous growth of phases in thin films poses a challenge that still needs to be resolved. The usual explanation [15] for the sequential growth that is normally observed in thin film systems is that there exists a critical thickness that one phase must attain before the growth of the next phase can become kinetically viable. For the second phase to nucleate and grow, the first phase must either exceed its critical thickness or at least one of the parent phases must be exhausted so that the first phase has no more material for growth, and becomes a material for second phase formation itself. In thin-film couples, the thickness of the deposited thin film layer is usually so small that the latter is the case. This results in a situation where phase growth follows a well-defined sequential pattern. In the event that the critical thickness of the first phase is so low that surplus materials are available after it (first phase) attains its critical thickness, it is possible for other phases to grow concurrently. Nemouchi *et al.* [10] therefore ascribed the simultaneous growth of Ni_5Ge_3 and NiGe observed in the Ni-Ge system to the low critical thickness of Ni_5Ge_3.

Figure 5 shows that the onset of NiGe formation was characterised by a drop in the growth rate of Ni_5Ge_3. There also appeared to be a change-over in the growth pattern from a parabolic to a linear fashion. It can also be noticed from the figure that the growth of NiGe started out on a very slow note and became rampant as soon as all the Ni was consumed. Habanyama *et al.* [3] made a similar observation and attributed it to ‘phase competition’ that

ensued between Ni_5Ge_3 and NiGe during the period of simultaneous growth. The phase competition favored the growth of Ni_5Ge_3; the growth of NiGe was limited because the Ni atoms had to first diffuse through the bulk of the Ni_5Ge_3 layer before they could reach the reaction interface to react with the Ge. Thus, the growth of NiGe only became prominent after complete consumption of Ni and commencement of the decomposition of Ni_5Ge_3.

2. Growth Kinetics

Using a Kissinger plot, which is a plot of $ln(x^2/T^2)$ against $1/T$, an estimation of the activation energy was obtained from the slope. The data for the Kissinger plot were taken in the temperature windows 151 – 216 ^oC and 235 – 254 °C for Ni_5Ge_3 and NiGe respectively. These temperature ranges were chosen so as to avoid the period of simultaneous growth where the analysis would have been complicated. The activation energy of diffusional growth of Ni_5Ge_3 was estimated to be $E_a = 0.83 \pm 0.05$ eV while that for NiGe was found to be $E_a = 1.33 \pm 0.05$ eV.

Previous studies that attempted to determine the activation energy of diffusional growth for the phase Ni_5Ge_3 include those by Nemouchi *et al.* [10] and Habanyama *et al.* [3]. Nemouchi *et al*. found that the activation energy of growth for Ni_5Ge_3 was 0.8 *eV* while Habanyama *et al*. found it to be 0.77 *eV*. The result obtained in the present study vis-à-vis the activation energy of growth of Ni_5Ge_3 is therefore in close agreement with the published literature. Meanwhile, experiments by Patterson and others [11] found the activation energy of diffusional growth of NiGe to be about 1.3 *eV*, almost in absolute agreement with the result obtained in this study.

LATERAL DIFFUSION COUPLE RESULTS

The lateral diffusion couples prepared with thick Ni islands on thin Ge films showed very limited lateral diffusion upon annealing. The reaction did not proceed beyond a certain point despite annealing at higher temperatures and for longer times, and left a Ge depletion layer around the edge of the island. On the other hand, the set of samples prepared with thick Ge islands on thin Ni films exhibited extensive lateral diffusion. It was on this set of samples that systematic analysis using SEM, AFM, and Nuclear Microprobe was performed. For presentation, we showcase results from the sample that was annealed at 500 °C for 2 hours.

A. SEM Results

Figure 6 shows an SEM micrograph of the sample that was annealed at 500 °C for 2 hours. The darkened rectangular area at the bottom end of the island is the area that was scanned with the microprobe and will be discussed later. The image on the right in Figure 6 is a closer view of the reaction zone of the sample shown on the left. Five distinct regions of varying brightness, labeled A-E, are observed. Regions A and E are the original Ge island and Ni thin film materials respectively, while regions B-D are the regions that were formed laterally as a result of heat treatment. The difference between regions C and D is arguable at first sight, but upon closer examination, it can be noticed that region C is brighter with fine grains, while region D is darker and becomes coarser as one moves outward. There is no well-defined boundary between the two regions.

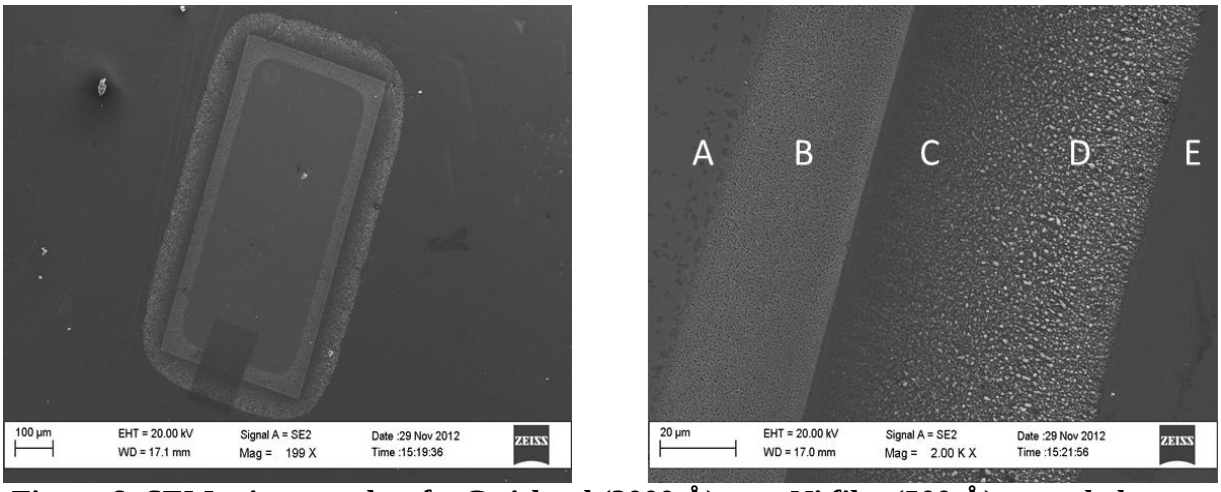

Figure 6: SEM micrographs of a Ge island (2000 Å) on a Ni film (500 Å) annealed at 500 °C for 2 hours. The micrograph on the left shows the whole sample while the one on the right zooms into the reaction zone to show the distinct regions more clearly.

B. AFM Results

Samples were scanned with an Atomic Force Microscope (AFM) to obtain further information pertaining to surface morphology and topography. The maximum lateral distance that could be covered in a single scan was 100 µm. In the event that the reaction zones were too large to be covered in a single scan, adjacent regions were scanned separately. The sample that was prepared with thick Ge islands on a thin Ni film and annealed at 500 °C for 2 hours was scanned over three different regions. The top picture in Figure 7 shows AFM images that were taken from adjacent regions on the reaction zones. Plots showing the depth profile across the reaction regions A-E are indicated beneath the images. The five reaction zones A-E identified with SEM are also observable with AFM. From the figure, region A appears to have a smoother microstructure than region B. Small and fine grains are observed in region C which progressively become larger and coarser, giving rise to the completely different microstructure observed in D. Here too, there is no clear-cut boundary between regions C and D.

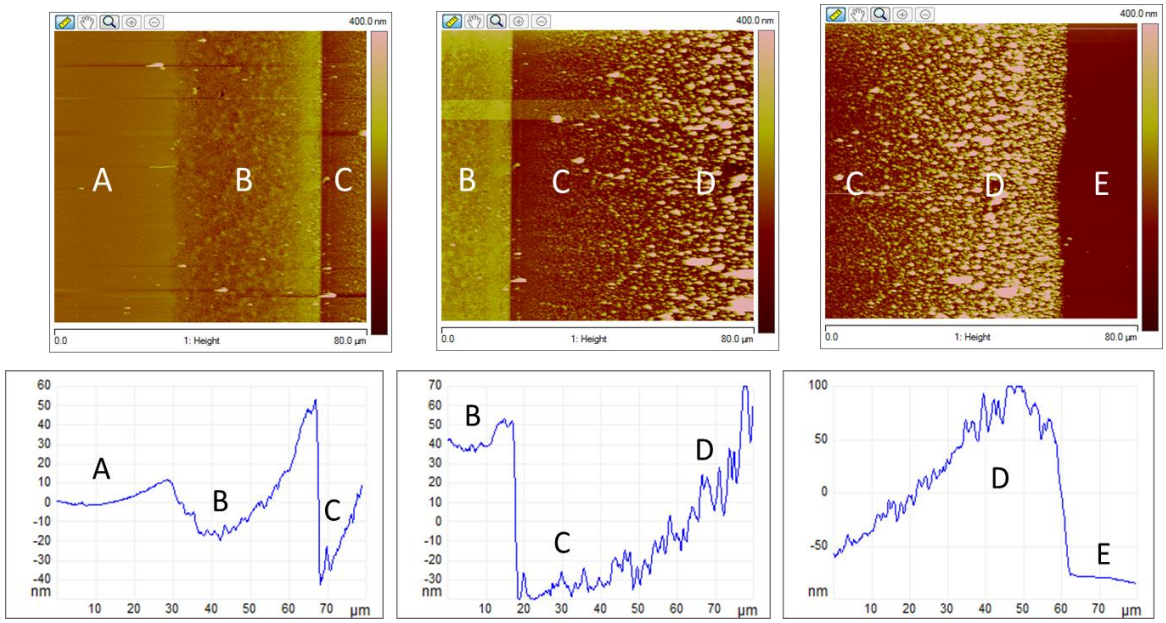

Figure 7: (Top) AFM images of the reaction zones of an island on the sample with Ge islands (2000 Å) on Ni thin films (500 Å) annealed at 500 °C for 2 hours. The five different regions identified are labelled A-E. (Bottom) Depth profiles across the scanned regions.

C. Microprobe RBS Results

A gradual deposition of carbon on the scanned area was one undesirable characteristic of the Nuclear Microprobe. This feature however turned out to be useful in this work as the scanned area was darkened (by the carbon) and hence easily identifiable in optical and SEM micrographs. The area that was scanned by the microprobe on the sample annealed at 500 °C for 2 hours is seen as a darkened rectangle in Figure 6. As can be seen, the scan covered all the distinct zones that were optically observed. Figure 8 shows representative RBS spectra from each of the five regions A-E. As expected, the film in region E consist solely of Ni, while the germanium content of the film in the remaining regions increases as one moves from D to A. It can also be noted that the spectrum from region D has a 'tail' (on its lagging edge) signifying that the surface there was rough.

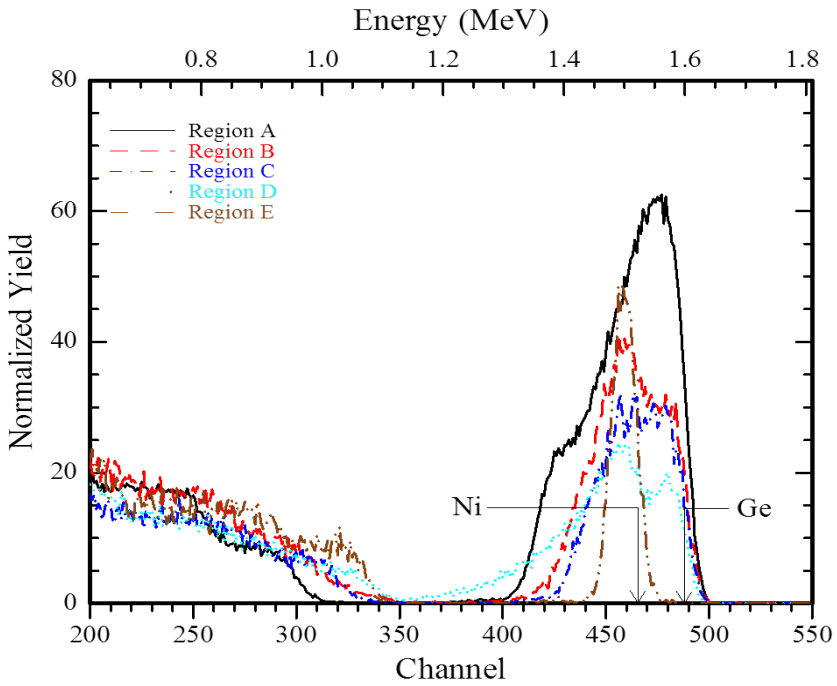

Figure 8: Superposition of representative RBS spectra from each of the five regions of the sample annealed at 500 °C for 2 hours. Also shown in the figure are the surface positions of Ni and Ge.

By setting 'energy gates' over selected channel intervals, RBS elemental maps were obtained. Excessive peak overlap made it difficult to select an energy gate that captured only backscattered counts from one atomic species secluding those from the other. Figure 9 shows the RBS map that was obtained by setting the energy gate over the channel range 403 – 416. This channel range corresponds to backscattered counts from the Ni atoms that were not at the surface of the sample. In the figure, the five reaction zones that were observed with other imaging techniques are clearly visible. The distinction between regions C and D, which was not so apparent with the other imaging techniques, is very eminent.

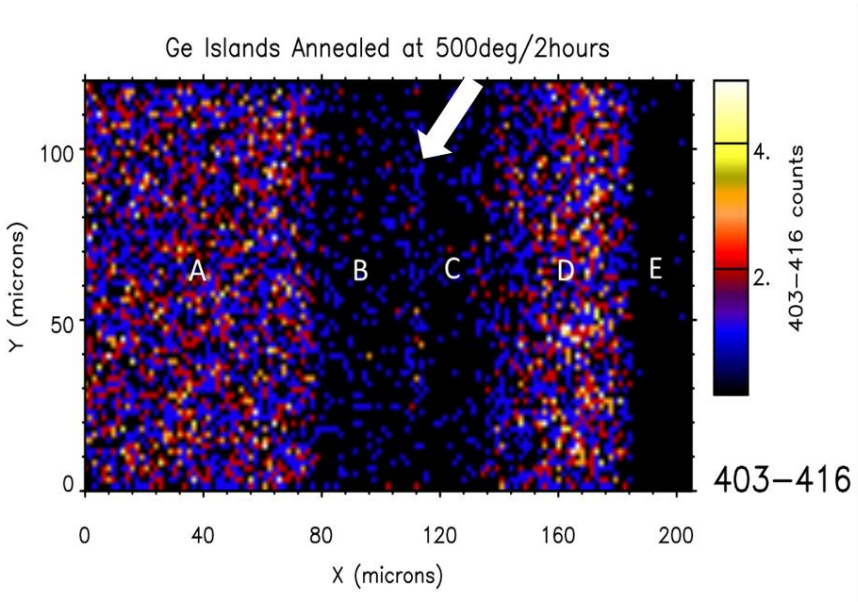

Figure 9: RBS map obtained when the gate was set between channels 403 and 416. The five different regions A-E are clearly visible. The arrow indicates the position of the original island/thin-film interface.

The backscattered counts registered in region A entail that the Ni atoms that were present in that region were not at the surface, but rather buried underneath a certain phase. This phase would most likely be Ge because it was supplied in excess in the island region. The phase underneath unreacted Ge is expected to be NiGe since it is the most Ge-rich phase in the Ni-Ge binary phase diagram. Hence, a situation is envisaged where unreacted Ge overlays NiGe in region A. In regions B and C, very few counts were observed. This means that the germanides that were formed in these regions were on the surface of the sample. The results obtained in region D seem to suggest that the Ni in that region was not at the surface of the sample. This was however not the case as the RBS counts observed in this region were because the phase that had formed there was rough, so that the Ni in thick regions could appear well below the surface. This was also confirmed by AFM (refer to Figure 7) which showed that the phase that had formed in region D is very fuzzy. Therefore, the counts that were observed in this region represent the Ni yield that was observed as a 'tail' in the spectrum extracted from this region (see Figure 8).

Simulation of spectra extracted from the reaction zones by RUMP revealed that regions D, C and B consisted of Ni_5Ge_3, Ni_3Ge_2 and NiGe respectively, while region A comprised NiGe overlaid by unreacted Ge.

D. Microprobe PIXE Results

It was demonstrated by Habanyama *et al.* that PIXE could compliment RBS in studies of lateral diffusion systems that exhibit excessive RBS peak overlap. Ever since, no work on the application of PIXE in a lateral diffusion couple study has been reported. This work is the first to use PIXE systematically in studying a lateral diffusion system.

Figure 10 shows the total PIXE spectrum (plotted as a green line) that was obtained from the scanned area of the sample annealed at 500 °C for 2 hours. A Dynamic Analysis matrix

for the PIXE spectrum was generated using the GeoPIXE II software package and projected as a map representing the elements present in the scanned area.

The map constructed from Ge-L X-rays showed more clearly the elemental distribution than the maps from other lines, and is displayed in Figure 11. After careful analysis of the dimensions of the area that was darkened by the carbon-deposition, it was found that the original interface actually corresponded to the position indicated by the white line in the PIXE map of Figure 11. The five distinct regions, observed with other imaging techniques, are also discernible with PIXE. Whereas optical microscopy and SEM showed lucidly the boundary between regions B and C, PIXE could not resolve it very clearly.

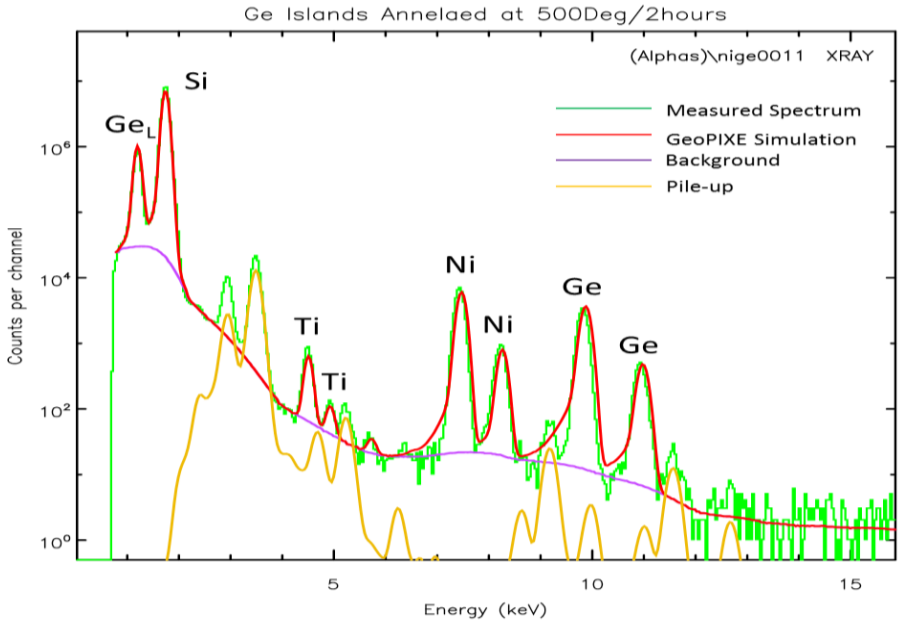

Figure 10: Total PIXE spectrum of the entire area scanned by the ion beam.

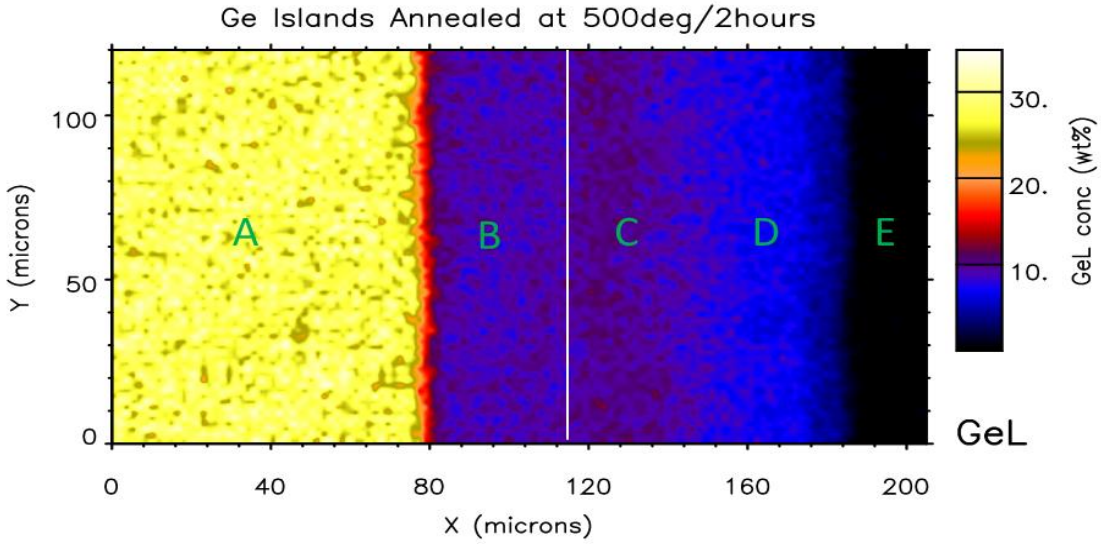

Figure 11: PIXE map showing the concentration of Ge atoms in the scanned region. The legend to the right gives the colour code.

E. Analysis and Discussion (Lateral Diffusion Couples)

The five different imaging techniques (optical microscopy, AFM, SEM, RBS, PIXE elemental imaging) employed in this study all agreed on the presence of five distinct reaction zones on the annealed samples consisting of Ge-island on thin Ni films. These regions were labelled A-E. Since A and E were the original Ge island and Ni thin film respectively, only three reaction zones (B-D) had effectively formed (laterally) as a result of heat treatment. Analysis using the nuclear microprobe revealed that these reaction zones respectively consisted of NiGe, Ni_3Ge_2, and Ni_5Ge_3. NiGe, together with a small portion of the Ni_3Ge_2 phase was entirely located inside the original island while Ni_5Ge_3 and the larger part of Ni_3Ge_2 were found outside the original interface. Figure 12 shows schematically the different phase regions observed as well as the various parameters used to characterise phase growth using the modified model of Gösele and Tu [16]. The subscripts α, β and γ refer to the phases NiGe, Ni_3Ge_2 and Ni_5Ge_3 respectively, while widths of the respective phase regions are represented by X_α, X_β and X_γ. Reaction interfaces between the different phases are denoted by $X_{\alpha\beta}$, $X_{\beta\gamma}$ and $X_{\gamma Ni}$ respectively. The phase regions on the extreme ends represent the state of the system before the beginning of lateral interactions.

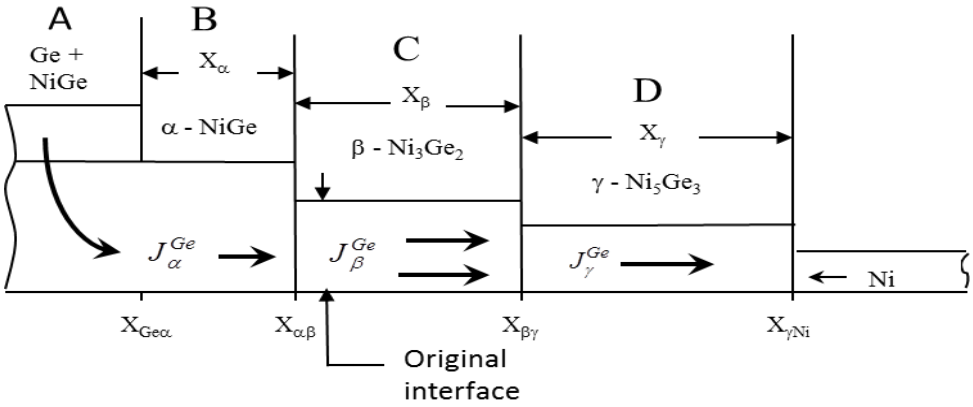

Figure 12: Diagram showing different phase regions and the various parameters used to characterise growth kinetics using the modified model of Gösele and Tu [16].

After thorough consideration of all the lateral diffusion couple results obtained using different techniques, phase formation and growth kinetics in the Ni-Ge system can be summed up in the following manner:

Upon annealing, interfacial interactions took place in the island region between Ge and Ni atoms in the underlying thin film, transforming the system through to its last phase NiGe (in the thin film regime). The interfacial reactions consumed all the Ni directly beneath the island but left some unreacted Ge, since Ge was supplied in excess. Thus, at the end of interfacial reactions, a situation is envisioned where the source region consisted of NiGe covered with unreacted Ge. As the annealing process continued, the unreacted Ge started diffusing out of the island and reacting with the surrounding Ni in the thin film region to form Ni_5Ge_3. The Ge that diffused out of the source region left exposed the NiGe that had formed during the interfacial stage of the reaction, giving rise to the visibly distinct region observed in region B. As the reaction proceeded, the region of exposed NiGe grew to an extent where the Ge flux at the reaction interface $X_{\gamma Ni}$ could no longer sustain the formation of Ni_5Ge_3. At this point, exposed NiGe started to decompose through the mechanism

$$3NiGe \rightarrow Ni_3Ge_2 + Ge$$

The decomposition process not only introduced Ni_3Ge_2 in the reaction zone (region C), but also liberated some Ge atoms which complemented the Ge supply to reaction interfaces farther out. The natural consequence of the decomposition process should have been to decrease the width of exposed NiGe with increased anneal time. However, this was not the case; instead of shrinking with increased anneal time, the region of exposed NiGe continued to grow. The only plausible explanation for this observation is that depletion of unreacted Ge from the source region continued in parallel with NiGe decomposition, with the latter process proceeding at a slower rate.

Thus, unreacted Ge atoms in the source region diffused through NiGe with an atomic flux J_{α}^{Ge} towards the $X_{\alpha\beta}$ interface. Ge atoms from the decomposition reaction at this interface were added to this flux, resulting in J_{β}^{Ge} flowing through the phase Ni_3Ge_2. This flux 'fed' the reaction at the $X_{\beta\gamma}$ interface where Ni_5Ge_3 was transformed to Ni_3Ge_2 through the mechanism

$$Ge + 3Ni_5Ge_3 \rightarrow 5Ni_3Ge_2$$

This reaction used up some Ge, thereby reducing the atomic flux from J_{β}^{Ge} to J_{γ}^{Ge}. It was the latter flux that furnished the reaction interface $X_{\gamma Ni}$ with Ge for further Ni_5Ge_3 growth. Table 2 shows a summary of the reactions that took place at each reaction interface.

Table 2: Equations of the reactions that take place at each interface.

Interface	Equation of Reaction
$X_{\alpha\beta}$	$3NiGe \rightarrow Ni_3Ge_2 + Ge$
$X_{\beta\gamma}$	$Ge + 3Ni_5Ge_3 \rightarrow 5Ni_3Ge_2$
$X_{\gamma Ni}$	$3Ge+5Ni \rightarrow Ni_5Ge_3$

To determine reaction kinetics, the increase in width of each reaction region was observed with anneal temperature and time. The interface between region B and C was distinct, making it possible to determine the average activation energy corresponding to the rate of exposure of NiGe, in competition with its rate of decomposition. Figures 13 - 15 show plots of reaction length against time for temperatures 500 °C, 400 °C, and 300 °C. It must be emphasised that the growth curves for the region labeled NiGe are due to both the exposure of NiGe by the consumption of overlaying Ge at the A-B interface and the decomposition of NiGe into Ni_3Ge_2 at the B-C interface.

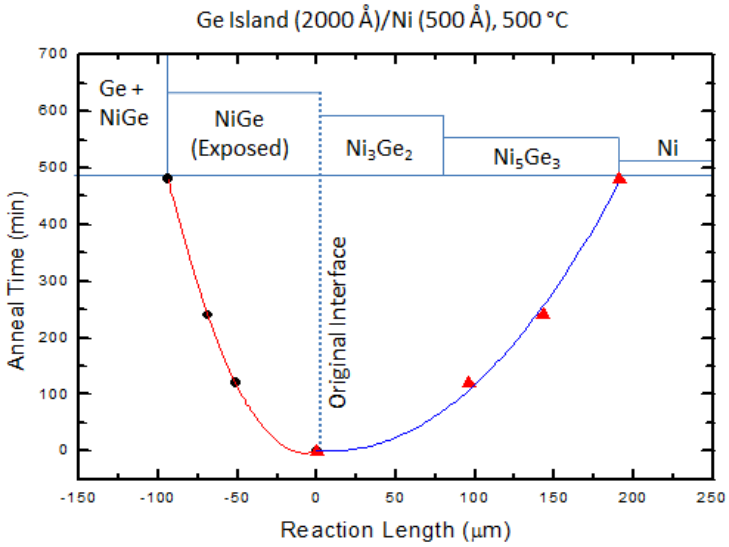

Figure 13: Plot of reaction length of individual germanide phases against anneal time for the samples annealed at 500 °C. The curve on the left of the original interface represents the rate of exposure of NiGe, in competition with its rate of decomposition, while the curve on the right of the original interface shows the time rate of 'combined' growth of the phases Ni_3Ge_2 and Ni_5Ge_3. A parabolic dependence of compound growth on anneal time is observed.

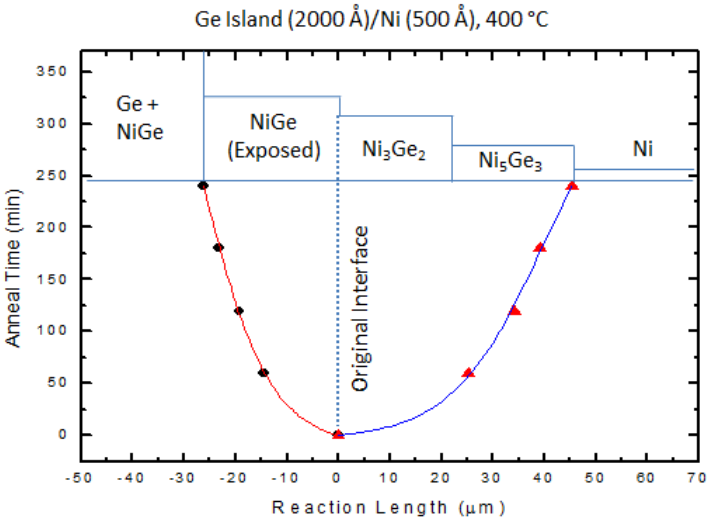

Figure 14: Plot of reaction length of individual germanide phases against anneal time for the samples annealed at 400 °C. The curve on the left of the original interface represents the rate of exposure of NiGe, in competition with its rate of decomposition. The curve on the right of the original interface shows the time rate of 'combined' growth of the phases Ni_3Ge_2 and Ni_5Ge_3.

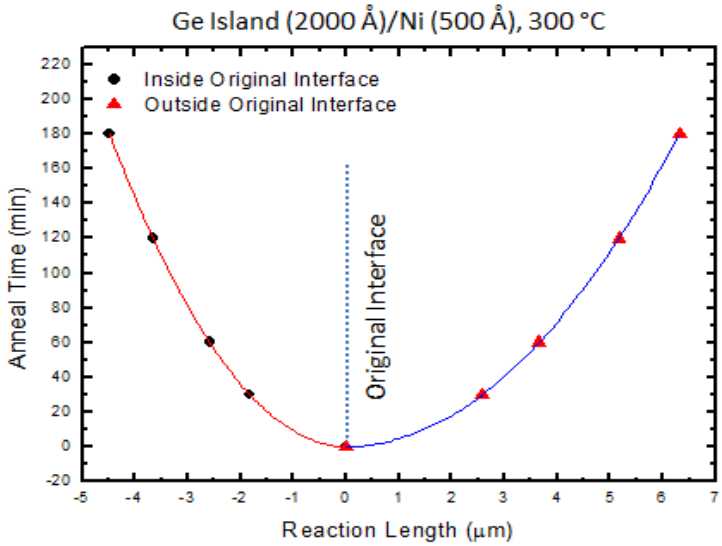

Figure 15: Plot of reaction length of individual germanide phases against anneal time for the samples annealed at 300 °C.

A parabolic dependence of compound growth on anneal time is observed. This is indicative of a diffusion-limited growth process which, as modeled by Kidson [17], results in parabolic growth even in multi-phase systems. Thus, the lateral growth of Ni_3Ge_2 and Ni_5Ge_3, and the exposure/decomposition of NiGe followed a diffusion limited process.

Squares of reaction length were plotted against anneal time. Reciprocals of the slopes of the straight lines obtained were calculated. These values represent the diffusional growth constants, $K_\beta = x_\beta^2/t$. The logarithm of K_β (for each annealing temperature) was plotted against the reciprocal of the product of the Boltzmann constant and the absolute temperature $(1/k_BT)$ in the Arrhenius plot shown in Figure 16. From the slope of this plot, the activation energy of diffusional growth for the combined lateral growth of Ni_3Ge_2 and Ni_5Ge_3 was determined and its value found to be 0.9 ± 0.1 eV. Using a similar procedure, the average activation energy corresponding to the rate of exposure of NiGe, in competition with its rate of decomposition, was determined to be 1.1 ± 0.1 eV. The results are shown in Figure 17.

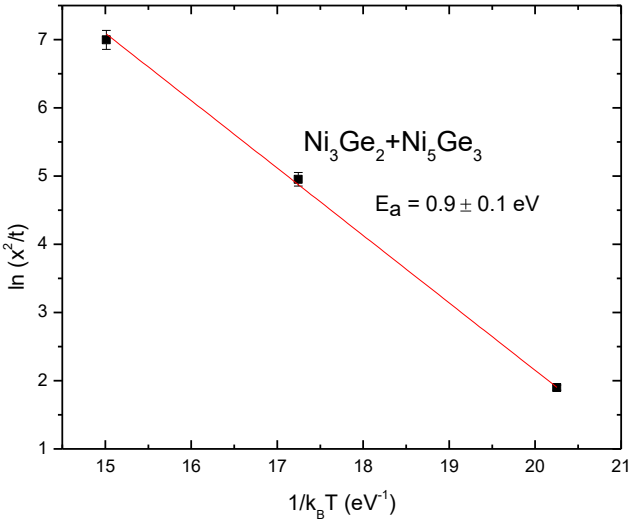

Figure 16: Arrhenius plot of the combined lateral growth rates of Ni_3Ge_2 and Ni_5Ge_3, yielding an activation energy of 0.9 ± 0.1 eV.

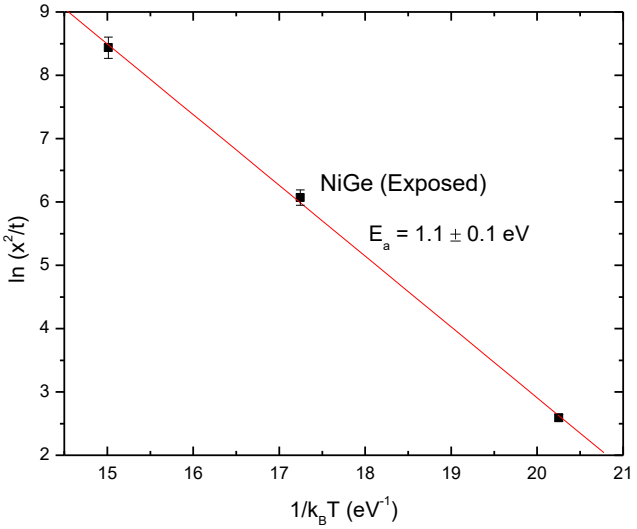

Figure 17: Arrhenius plot of the rate of exposure of NiGe, in competition with its rate of decomposition. The value of the average activation energy was found to be 1.1 ± 0.1 eV.

CONCLUSIONS

In thin-film couples, two of the nine phases predicted in the Ni-Ge phase diagram were observed, *viz.* Ni_5Ge_3 and NiGe. The phases were formed in the sequence: Ni_5Ge_3, and then NiGe. Although formation of Ni_5Ge_3 started during deposition, its growth as a result of heat treatment only commenced around 150 °C. NiGe started to grow at 223 °C even before all Ni was consumed, resulting in a short period of co-existence of Ni_5Ge_3 and NiGe in the presence of unreacted Ni. After complete consumption of Ni at 232 °C, Ni_5Ge_3

decomposed as NiGe grew at its expense. The reaction stopped at 254 ^{0}C when all Ni_5Ge_3 was consumed.

In lateral diffusion couples, three different compound phases, *viz.* NiGe, Ni_3Ge_2 and Ni_5Ge_3, were observed in the samples with Ge islands on Ni thin films. The NiGe and Ni_5Ge_3 regions were respectively located inside and outside the original island boundary while the Ni_3Ge_2 region stretched across the boundary, with more of it being outside. It should be noted that the germanides spread out from the source region in their decreasing order of germanium content, as expected.

ACKNOWLEDGMENTS

The authors would like to thank the Department of Physics at the University of Zambia, under Energy and Environment Research Group (EERG) in conjuction with Uppsala University of Sweden for sponsoring this research project. Many thanks are also due to the staff at the Materials Research Department of iThemba LABS, Faure for their kind assistance and co-operation in all aspects of the experimental measurements. We thank the National Research Foundation for their financial support for this work.

REFERENCES

1 S. Gaudet, C. Detavernier, C. Lavoie, and P. Desjardins, J. Appl. Phys. **100** 034306 (2006).
2 F. Nemouchi, D. Mangelinck, J.L. Lábár, M. Putero, C. Bergman, and P. Gas, Microelectron. Eng. **83**, 2101 (2006).
3 A. Habanyama, C.M. Comrie, and K. J. Pondo, Afr. Rev. Phys. **6**, 87 (2011).
4 C.M. Comrie, K.J. Pondo, C. van der Walt, D. Smeets, J. Demeulemeester, A. Habanyama, W. Knaepen, C. Detavanier, and A. Vantomme, Thin Solid Films **526**, 261 (2012).
5 E. D. Marshall, C. S. Wu, C. S. Pai, D. M. Scott, and S. S. Lau, Mater. Res. Soc. Symp. Proc. **47**, 161 (1985).
6 L. J. Jin, K. L. Pey, W. K. Choi, E. A. Fitzgerald, D. A. Antoniadis, A. J. Pitera, M. L. Lee, D. Z. Chi, and C.H. Tung, Thin Solid Films **462-463**, 151 (2004).
7 Y.F. Hsieh, L.J. Chen, E.D. Marshall, S.S. Lau, and N. Kawasaki, Thin Solid Films **162**, 287 (1988).
8 M. Wittmer, M.A. Nicolet, and J.W. Mayer, Thin Solid Films **42** 51 (1977).
9 S Gaudet, U Detavernier, Christophe Gent, C Lavoie, and P Desjardins, J. Appl. Phys. **100** (3), 034306 (2006).
10 F. Nemouchi, D. Mangelinck, C. Bergman, G. Clugnet, and P. Gas, Appl. Phys. Lett. **89**, 131920 (2006).
11 J. Ken Patterson, B.J. Park, K. Ritley, H.Z. Xiao, L.H. Allen, and A. Rockett, Thin Solid Films **253** (1-2), 456 (1994).
12 M. Mueller, Q.T. Zhao, C. Urban, C. Sandow, D. Buca, S. Lenk, S. Estévez, and S. Mantl, Mater. Sci. Eng. B **154-155**, 168 (2008).
13 S Gaudet, C Detavernier, A. J Kellock, P Desjardins, and C Lavoie, J. Vac. Sci. Technol. A **24**, 474 (2005).
14 Y.F. Hsieh, L. J. Chen, E. D. Marshall, and S. S. Lau, Appl. Phys. Lett. **51** (20), 1588 (1987).
15 U. Gösele and K.N. Tu, J. Appl. Phys. **53** (4), 3252 (1982); W. C. Johnson and G. Martin, J. Appl. Phys. **68** (1990); F.M. d'Heurle, J. Mater. Res. **3**, 167 (1988).

[16] B. Blanpain, J. W. Mayer, J. C. Liu, and K. N. Tu, J. Appl. Phys. **68**, 3259 (1990);
B. Blanpain, J W mayer, J. C. Liu, and K. N. Tu, Phys. Rev. Lett. **64**, 2671 (1990).
[17] G.V Kidson, J. Nucl. Mater. **3**, 21 (1961).